Colloid Polym Sci (2008) 286:999–1007
DOI 10.1007/s00396-008-1862-6

ORIGINAL CONTRIBUTION

Behavior study of polyvinyl alcohol aqueous solution in presence of short chain micelle-forming polyols

Christine Damas · Timothée Leprince · Thi Huong Viet Ngo · Robert Coudert

Received: 16 November 2007 / Revised: 4 March 2008 / Accepted: 4 March 2008 / Published online: 24 May 2008

Abstract Interactions in aqueous solution between polyvinyl alcohol (PVA) and various short chain nonionic polyols surfactants having six to nine carbon atoms and two to three hydroxyl groups are investigated using tensiometry, viscosity, and dynamic laser light scattering techniques. Despite the fact that weak interactions are noticed, they begin to occur at surfactant concentrations far lower than the Critical Micellar Concentration. Partition coefficients of the surfactants between water and the PVA macromolecules are determined, and the contributions of the surfactant alkyl chain length on one hand and of the hydroxyl groups on the other hand to the PVA interactions with monomer surfactants are discussed in terms of thermodynamic contributions.

Keywords Nonionic polymer surfactant interactions · Viscosity · Surface properties · Dynamic light scattering

Introduction

Polymers and surfactants in aqueous solutions attract interest in a broad field of practical applications as well as in fundamental research. They are frequently present in areas such as pharmaceutical formulations, detergents, personal care products, foods, paints, and petroleum recovery. A lot of research has been focused on the field of polymer–surfactant interactions. The ability of polymer and the surfactant molecules to influence the solution and interfacial characteristics is controlled by the state of their occurrence in aqueous solutions, namely whether they form mixed aggregates in solution and, if so, the nature of their microstructures. Polymer–surfactant association is influenced by many factors such as their ionic or nonionic character, the hydrophobicity of the polymer, and of the surfactant tail or the presence of additives [1–3]. Most studies focus on complexes of anionic surfactants with polymers such as polyethylene oxide (PEO) or polypropylene oxide (PPO). In general, nonionic polymers interact strongly with anionic surfactants [4–6] but weakly with cationic surfactants [7], whereas ionic polymers interact with surfactants of opposite charge [8, 9]. Moreover, the existence of complex formation between anionic surfactants and anionic polymers which has been reported [10] shows the importance of the hydrophobic attraction. In the case of uncharged polymer and charged or uncharged surfactant, the differences observed in the interaction strengths are connected to the hydrated size of the surfactant head group, which is larger for the rather bulky cationic or nonionic surfactants compared to the anionic ones. For systems with nonionic components, interactions are generally considered to be very weak [11]. Recently, some studies suggest that there is a significant interaction in aqueous neutral polymer and nonionic surfactant systems such as polyethylene oxide nonyl phenyl ether with hydroxyethylcellulose or PEO, and *n*-octylthioglucoside with PPO or hydroxypropylcellulose. However, all studies involve surfactants with long alkyl chain length as hydrophobic part [12].

As further evidence for the existence of neutral polymer–surfactant complexes and to extend the polymer surfactant interactions investigation to the case of short chain nonionic surfactants, we have focused the aim of the present work on

C. Damas (✉) · T. Leprince · T. H. V. Ngo · R. Coudert
Département de Chimie,
Laboratoire de Chimie des Interfaces et des Milieux Electrolytiques-CIME-EA 2098, Université de Tours,
Parc Grandmont,
37200 Tours, France
e-mail: damas@univ-tours.fr

systems involving a neutral polymer having hydroxyl groups such as polyvinyl alcohol (PVA) with polyol surfactants. PVA is produced commercially on a large scale and is used in various industrial applications as emulsifying, coating, or adhesive agent and also in medical applications as a material for drug-delivery systems and the immobilization of enzymes [13–16]. In water, there exist two possible intermolecular interactions among PVA chains or between PVA and water, as follows: H-bonding between hydroxyl groups on PVA chains and H-bonding between the –OH groups of PVA and water molecules. Upon addition of small water-soluble molecules such as surfactants, the composition and physico-chemical characteristics of the new aqueous solvent are modified from a homogeneous mixture of surfactants monomers and water to an aqueous colloidal medium where micellar aggregates coexist with monomer surfactants in water as the surfactant concentration becomes higher than the Critical Micellar Concentration (CMC). Thus, the degree of polymer solvent interaction can be significantly affected by a change in the aqueous solvent characteristics, which can modify simultaneously the properties of polymer solutions. For systems involving PVA with short chain micelle-forming polyols such as 1,2-hexanediol (HD), 1,2,3-heptanetriol (HpT), 1,2,3-octanetriol (OT), and 1,2,3-nonanetriol (NT), H-bonding interactions may take place not only between macromolecules or between macromolecules and water but also with polyols. Moreover, hydrophobic interactions between polyols and the PVA hydrocarbon skeleton should be also taken into consideration. Hence, the PVA aqueous polyol solution behavior is compared to systems involving short chain monoalcohols. Owing to previous studies [17, 18] about the influence of short chain monohydric alcohols on PVA behavior, the alcoholic aqueous solution behavior of PVA depends firstly upon the concentration of added alcohol and secondly on the structure of the alcohol. The more hydrophobic the alcohol is, the more the effect is at low alcohol concentration.

This article deals with the investigation of PVA interactions with polyol aqueous solvents by viscosity measurements, dynamic laser light scattering, and tensiometry in order to clarify the influence of the polyol structure.

Experimental section

Materials

PVA was purchased from Merk–Schuchardt with a hydrolysis degree higher than 98% and was used as received. HD was purchased from Aldrich (with purity higher than 98%) and purified by distillation under reduced pressure (100–102 °C/4 mm Hg) before use. All triols HpT, OT, and NT were synthesized from the corresponding 1-alkene-3-ol with the method of Swern et al. [19] previously applied to those compounds in [20, 21]. The triols were purified by crystallization in various mixtures of ether and CCl_4 (80% (*v*/*v*) for HpT, 20% (*v*/*v*) for OT, and pure ether for NT). The purity (higher than 98%) was checked by G.C. or elemental analysis and infrared spectra.

Preparation of solutions

Aqueous polyol solutions are first prepared using deionized water with specific conductivity less than 8.10^{-6} S cm^{-1}. Such solutions are then used as solvents to prepare aqueous PVA or polyol solutions. The PVA powders were dissolved in the aqueous polyol solutions by heating to at least 80 °C for 4 h.

Methods

Intrinsic viscosity measurements were generally carried out at 30 °C or 45±0.1 °C using an Ubbelhode viscometer having an internal diameter of 0.53 mm (or 0.36 mm in the case of pure HD aqueous solutions and aqueous PVA solutions at 25 and 30 °C). In order to avoid any aging effects of PVA solutions, flow time measurements have been made on fresh solutions in less than 48 h. All the solutions and solvents are filtered through 0.45 μm pore size membranes before introduction in the viscometer. The solutions are prepared starting from an initial stock solution successively diluted in the viscometer. Each run time is repeated five times to give flow time measurements with an accuracy of 0.05 s. Hence, the measured flow time of water at 45 °C is 120.75±0.05 s. Kinetic energy corrections are made to the solvent, and the dilute solutions measured flow times (t_{mes}) to give the corrected flow times t according to: t (in seconds)$=t_{mes} - A/t_{mes}^2$ where A=30,607 s^3 or 70,500 s^3, respectively, for viscometers of 0.53 or 0.36 mm internal diameter. The reduced viscosity η_{red} of the polymer solutions is defined by $\eta_{red} = (\eta - \eta_0)/(\eta_0.C)$ where η and η_0 are respectively the absolute viscosities of the polymer solution and of the solvent, and C is the polymer weight concentration. From the corrected flow times of the polymer solution (t) and of the solvent (t_0), the reduced viscosity can be expressed as $\eta_{red} = (t - t_0)/(t_0.C)$ for dilute ($C \leq 1$ g/100 mL) and Newtonian polymer solutions. Also, the reduced viscosity can vary with C according to the Huggins [22] equation $\eta_{red} = [\eta] + k_H[\eta]^2 C$ or to the Kraemer [23, 24] equation $\frac{\ln \eta_r}{C} = [\eta] - k_K[\eta]^2 C$, where $\eta_r (= \eta/\eta_0 = 1 + \eta_{red}.C)$ is the relative viscosity, $[\eta]$ is the intrinsic viscosity which is related to the specific volume of the macromolecular species present in the solution, and k_H and k_K are respectively the Huggins and Kraemer coefficients with $k_H + k_K = 1/2$

The surface tension γ was measured with an accuracy of 0.1 mN/m by the De Nouy ring method using a K10ST Krüss digital tensiometer. A sample cell with constant temperature (±0.1 °C) water passing through its jacket is used. The surface tension was measured for binary surfactant water systems and for ternary surfactant–PVA–water systems. For the latter systems, the PVA concentration was kept constant at 0.5% *w/w*.

Dynamic light scattering The light scattering apparatus was from Malvern, model 4700. The optical source of the light-scattering apparatus (Coherent Company, Model Innova-70C) is an argon–ion laser operating at 488.0 nm with an output power of 2 W maximum. The filtered solution (through 0.2 μm pore size membrane) is placed in a cylindrical cell immersed in an index matching liquid bath to avoid reflections. The liquid is thermostated at 30.0 ± 0.1 °C. Measurement of the time dependent correlation function of the scattered intensity is made at a scattering angle of 90°. The autocorrelation function is, then, analyzed by the method of cumulants [25] and the hydrodynamic diameters of the aggregates are obtained from the apparent diffusion coefficients using the Stokes–Einstein relationship: $D_{h,0} = k_B T / 3\pi\eta D_{t,0}$, where k_B is the Boltzmann constant, T the absolute temperature, η the viscosity of the continuous medium and $D_{t,0}$ the value of the translational diffusion coefficient D_t extrapolated at zero polymer concentration according to: $D_t = D_{t,0}[1+k_D C]$ where k_D is the hydrodynamic virial coefficient.

Results and discussion

PVA–water and polyol–water binary systems

The aqueous solution properties of such systems have been extensively studied in the literature. The ability of 1,2,3-alkanetriols to micellize has been previously investigated [21]. The results indicate the onset of micellization for HpT, OT, and NT at the respective CMCs 0.98, 0.32, and 0.10 mol.L^{-1} at 40 °C. The CMC decrease in the order HpT, OT, and NT is in good agreement with the increase of the hydrophobic character through the alkyl chain length. At the same temperature, the CMC of HD lies between 0.47 and 0.73 mol L^{-1} [26]. HD presents the same alkyl chain length as HpT ones but a weaker polar head. Its CMC should be then lower than that of HpT, which is effectively noticed. Dynamic light scattering experiments lead to hydrodynamic diameters D_h of the micellar aggregates. Linear extrapolation of the diffusion coefficient vs. surfactant concentration to zero micellar aggregates (or CMC) leads to $D_{h,0}$=2.98 nm for HD at 30 °C (see Fig. 1a), which is quite close to the value obtained in previous studies—2.70 nm at 20 °C [27]. Similarly, the $D_{h,0}$ values of HpT and OT are respectively 3.72 and 4.06 nm (found 3.88 nm for OT at 20 °C in [27]).

PVA is known to solubilize more or less easily in water, owing to the degree of hydrolysis of the poly(vinylacetate) precursor polymer [28]. At degrees of hydrolysis higher than 98%, PVA is highly crystalline and form strong interchain or intrachain hydrogen bonding. Then, its solubility in water is strongly affected, and a solubilization temperature above 80 °C is required to dissolve PVA completely. Upon cooling, PVA remains in solution. Its storage time does not exceed 2 days to avoid the formation of aggregates.

The PVA sample used in the present study was characterized using intrinsic viscosity measurements to determine its average molar mass $\overline{M_j}$ where the subscript j stands for viscosity (j=v) or weight (j=w) average. The intrinsic viscosity [η] is determined by extrapolating linearly the variation of the reduced viscosity η_{red} with the PVA weight concentration C to zero polymer concentration, as shown on Fig. 2. For accuracy, the second method based on the extrapolation to zero polymer

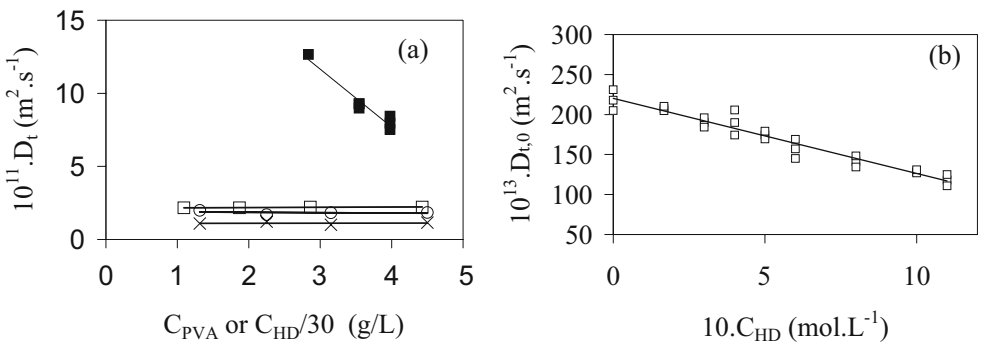

Fig. 1 Variations of the (PVA or HD) translational diffusion coefficient D_t (**a**) with PVA weight concentration (C_{PVA}; in pure water: *white squares*; in aqueous solution with HD at 0.5 mol L^{-1}: *white circles*; in aqueous solution with HD at 1.1 mol L^{-1}: *crosses*) or with HD weight concentration (C_{HD}) in water (*dark squares*), **b** $D_{t,0}$ (PVA diffusion coefficient D_t extrapolated at C_{PVA} = 0) with C_{HD} in HD–water solution at 30 °C

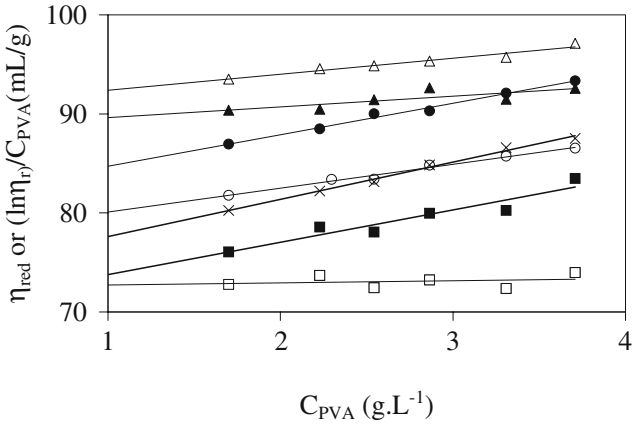

Fig. 2 Variations of the reduced viscosity η_{red} as a function of PVA weight concentration C_{PVA} in various media (*dark squares*: PVA in water at 45 °C; *crosses*: PVA in OT (0.12 mol L^{-1})–water at 45 °C; *white circles*: PVA in NT (0.12 mol L^{-1})–water at 45 °C; *dark circles*: PVA in HpT (0.47 mol L^{-1})/water at 45 °C; *dark triangles*: PVA in OT (0.47 mol L^{-1})–water at 45 °C; *white triangles*: PVA in HD (0.62 mol L^{-1})–water at 45 °C). The variation of $(\ln\eta_r)$–C_{PVA} with C_{PVA} is also shown for PVA in water at 45 °C (*white squares*)

concentration of $(\ln\ \eta_r)/C$ vs. C is also used to determine $[\eta]$. The $[\eta]$ values obtained from both methods are in good accordance.

The k_H values are quite constant around 0.64±0.01 in the temperature range 25–45 °C. Such values are shortly close to those obtained by Matsumoto et al. [28]. Although water is not a poor solvent for PVA, the k_H values are often higher than 0.5. This fact is attributed to a partial association of PVA macromolecules. According to [29], for a sample with $[\eta]$=82 mL/g, C=0.1 g/100 mL, and $\alpha\geq$ 0.98, a PVA association degree of 3% is estimated. Moreover, the degree of association should decrease with a molecular weight decrease. The intrinsic viscosity $[\eta]$ is linked to $\overline{M_j}$ according to the following Mark–Houwink relation: $[\eta] = K\left(\overline{M_j}\right)^a$ where K and a are function of polymer, solvent, and temperature.

From various values of K and a parameters of the literature listed in Table 1, and from the experimental $[\eta]$ values obtained in the present study, corresponding average molar masses are calculated. The calculated $\overline{M}_v$ values listed in Table 1 lead to a mean value of 66,300±13,100 g/mol. The $\overline{M}_w$value of 72,450 g/mol is calculated from parameters of [33]. The $\frac{\overline{M}_v}{\overline{M}_w}$ ratio is, then, equal to 0.915, which is in good accordance with the ratio predicted by the high polydisperse Schulz distribution [36] (polydispersity index = 2).

From dynamic light scattering experiments, diffusion coefficients D_t are determined at various polymer concentrations C_{PVA} at 30 °C. Extrapolation of D_t vs. C_{PVA} (see Fig. 1a) to zero polymer concentration gives $D_{t,0}$= $2.18.10^{-11}$ m^2 s^{-1} and the hydrodynamic radius at infinite dilution $R_{h,0}$=12.8 nm from the Stokes–Einstein law. An estimation of the viscosity radius R_v, which is quite close to R_h, can be undertaken from intrinsic viscosities and use of Einstein's law of viscosity which originally applied to extremely dilute dispersions of spherical particles, considering the spheres are large enough compared to the solvent molecules and small enough compared to the dimensions of the viscometer: $\frac{\eta}{\eta_0} = 1 + 2.5\ \phi$, where ϕ is the total volume fraction of the dispersed phase. The size restrictions make this result applicable to particles in the colloidal size range. This equation becomes at infinite polymer dilution: $[\eta] = 2.5\frac{V_m}{M}$ where M is the molar mass of the particles. V_m is the molar volume of the spheres and is identical to their effective flowing volume V_e defined in the Vand equation which has also been applied to PVA samples [18]: $\frac{\ln\ \eta_r}{C} = \frac{2.5V_e}{1-kC_mV_e}$ where C_m is the molar concentration of PVA monomer units. This equation becomes: $[\eta] = 2.5\frac{Ve}{M}$ at infinite polymer dilution. Application of this equation to the present PVA sample gives the corresponding viscosity radius (see Table 1): $R_v = \left(\frac{3[\eta]M}{10.\pi.N_A}\right)^{1/3}$ The R_v value (9.5 nm) at 30 °C can be compared to the R_h value (12.8 nm)

Table 1 PVA characteristics obtained from viscometric and dynamic light scattering measurements on PVA aqueous solutions at various temperatures

Temperature; [η] (mL/g); k_H	[Reference]: α[a]; K[b]; a[c]	$\overline{M}_j$ (g/mol)	R_v[d]; R_g[d]; R_h[e] (nm)
25 °C; 73.8±0.1; 0.65	[30]: 0.996; $6.03.10^{-2}$; 0.628	$\overline{M}_v$=82670	9.9; 11.4–12.6
	[30]: 0.98; $6.49.10^{-2}$; 0.621	$\overline{M}_v$=82650	9.9; 11.4–12.6
	[31, 32]: unknown; $2.0.10^{-2}$; 0.76	$\overline{M}_v$=49020	8.3; 9.5–10.5
30 °C; 73.4±0.1; 0.65	[33]:≥0.996; $6.51.10^{-2}$; 0.628	$\overline{M}_w$=72450	9.5; 10.9–12.0; 12.8
	[34]: unknown; $6.66.10^{-2}$; 0.64	$\overline{M}_v$=56730	8.7; 10.0–11.0
	[35]:unknown; $7.97.10^{-2}$; 0.62	$\overline{M}_v$=60400	8.9; 10.2–11.2
45°C; 72.1±0.4; 0.63			

[η] Intrinsic viscosities, R_v viscometric, R_g gyration, R_h hydrodynamic
[a] Degree of hydrolysis of the precursor polymer (poly(vinylacetate))
[b,c] Parameters of the Mark–Houwink equation for [η] expressed in mL/g
[d] Estimated
[e] Experimental

determined by dynamic light scattering. This leads to R_v/R_h ratio of 0.74. However, for linear polymer chains, theories predict R_v/R_h ratio ranging from 1.00 at the hard sphere limit to 1.036 in a nondraining good solvent and 1.075 at the theta condition [36]. Analogously to similar R_v/R_h values (ranging from 0.80 to 0.95) obtained in the case of branched polyethyleneimine [37], such a low ratio can be attributed to the high polydispersity index of the polymer sample examined. The R_v equation is also analogous to the Flory–Fox equation [38], which links the radius of gyration R_g to $[\eta]$:$R_g = \left(\frac{M[\eta]}{6^{3/2}\phi}\right)^{1/3}$, where ϕ is the Flory–Fox parameter ranging from 2.1 10^{23} to 2.8 10^{23} mol^{-1}. Such a range of ϕ values leads to the corresponding range of R_g values indicated in Table 1. The radius of gyration can be compared to the hydrodynamic radius in terms of the dimensionless parameter ρ: $\rho=R_g/R_h$ [39]. This ratio implies the plausible structures of polymers. For linear polymers in a good solvent, many experimental results verify that ρ has a value in the range 1.5–1.7, which is quite close to the theoretical value of 1.504 predicted for a random coil (Gaussian chain). For a hard sphere, it is 0.775. For the present PVA sample in water at 30 °C, we estimate ρ between 0.85 and 0.93. This low ρ value seems to indicate a lack of rotational freedom in the polymer and a high degree of stiffness of the chains.

PVA–polyol–water ternary systems

Dynamic laser light scattering experiments have been undertaken to estimate the effect of added polyol surfactant on the PVA hydrodynamic size. As shown on Fig. 1a, the addition of HD leads to a decrease of D_t whatever the PVA concentration used. In order to exclude interacting effects, we examine the effect of HD on the PVA translational diffusion coefficient ($D_{t,0}$) determined at zero polymer concentration. A decrease of $D_{t,0}$ upon addition of HD is also obtained as shown on Fig. 1b. Such a behavior is consistent with the occurrence of PVA macromolecules with HD. In the HD concentration (C_{HD}) range examined, $D_{t,0}$ varies linearly with C_{HD}, but no change is noticed at the CMC of HD (around 0.6±0.1 mol L^{-1}). It is probably due to the solvent viscosity effect which seems to predominate on $D_{t,0}$ variation with C_{HD}. Hence, we examine the corresponding hydrodynamic radii $R_{h,0}$ estimated from the Stokes–Einstein equation. The values are gathered in Table 2 with a mean error of 0.6 nm.

Despite the quite close values, two series of R_h values are noticed: the first one is comprised between 12.2 and 12.8 nm, and the second one slightly increases from 13.4 to 14.3 nm. The first values are very close to that of PVA in pure water. The second values are around 1 to 2 nm higher than the first ones and correspond to HD concentrations higher than the CMC (≥0.6 mol L^{-1}). Then, interactions are noticed between PVA and micellar HD but in a small extent. Moreover, as the HD concentration exceeds its CMC, two population sizes are detected by dynamic light scattering as shown on Fig. 3: PVA in weak interaction with HD, and HD micelles (at around 3 nm of diameter) which also seem to behave as a separate system.

Then, after examining at first the hydrodynamic radii of the systems involved, no strong interaction seems to happen in bulk solution. Figure 4 shows the surface tension variations of aqueous HD solutions (in pure water or in presence of PVA) with the HD concentration. The γ vs. lnC curve obtained in the case of HD in pure water presents two steps: a first linear decrease followed by a plateau at 26.6 mN m^{-1}; the intercept of the two parts corresponds to the CMC at 0.53 mol L^{-1}, which is in good accordance with previous results. In presence of PVA at fixed weight concentration 0.5% (*w*/*w*), the aspect of the γ vs. lnC curve changes.

In the absence of surfactant, the PVA or water solvent presents a surface tension of 53.0 mN m^{-1} due to the surface activity of PVA alone in pure water. The surface tension decreases upon addition of HD by keeping γ lower than the corresponding surface tension of HD in water at the same HD concentration. At C=28.5 10^{-3} mol L^{-1}, a reduction of the γ decrease is noticed up to C=122.8 10^{-3} mol L^{-1}, with an inflection point in this concentration range. Then, the γ decrease parallels that of HD in pure water, and a plateau is reached at C=0.52 mol L^{-1}. The inflection point lies between 5.5% and 23.6% of the CMC. The presence of an inflection point can be attributed to the association of HD with the PVA macromolecules in such an extent that saturation or equilibrium is reached. However, the presence of PVA does not disturb the formation of HD micelles as it has also been evidenced by dynamic light scattering. The association of PVA may occur through two possible interactions: H-bonding between –OH groups of both HD and PVA and hydrophobic interactions between the alkyl chain of HD and the hydrocarbon skeleton of PVA, knowing that intermolecular H-bonding may compete with intramolecular or water H-bondings. Increasing the

Table 2 Hydrodynamic radii of PVA at infinite PVA dilution in HD–water at various HD concentrations, C_{HD}, at 30 °C

C_{HD} (mol L^{-1})	0	0.17	0.30	0.40	0.50	0.60	0.80	1.00	1.10
$R_{h,0}$ (nm; ±0.6 nm)	12.8	12.4	12.7	12.2	12.7	13.4	13.5	13.6	14.3

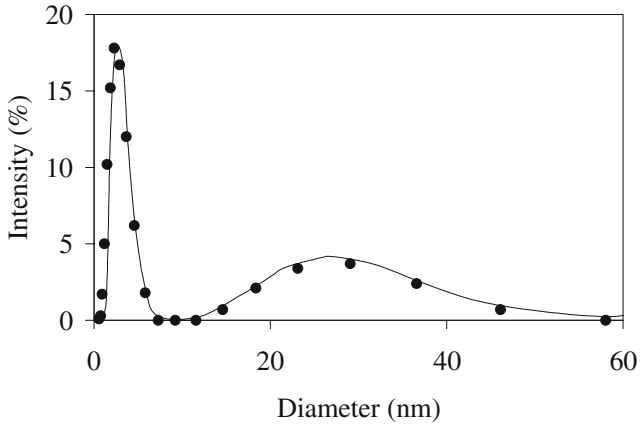

Fig. 3 Size distribution curve of the (PVA (4.5 g/L)–HD (1 mol L^{-1})–water) system at 30 °C, where the relative scattered intensity is reported as a function of the species diameter

alkyl chain length and the number of –OH groups in the nonionic surfactant may enhance such interactions. Thus, a similar study has been undertaken with NT. The γ vs. lnC curves are also shown on Fig. 4. The CMC of NT in pure water is 66.9 10^{-3} mol L^{-1}. In presence of PVA, the aspect of the curve is similar to that of the HD–PVA–water system, but for surface tensions lower than 43.5 mN m^{-1}, the surface tension remains higher than that of NT in pure water. The CMC remains unchanged at 66.8 10^{-3} mol L^{-1}. Moreover, the part of the curve covering the inflection point before the linear decrease down to the CMC point is quite short and less defined than in the case of the HD–PVA–water system. The inflection point occurs in the 3.5 10^{-3}–10.1 10^{-3} mol L^{-1} concentration range, which corresponds to 5.2% to 15.1% of the CMC. Similarly to HD–PVA–water systems, the interactions between NT and PVA in bulk solution occur far earlier than that of NT in micellar state. Examining the linear part of the γ vs. lnC curve after the inflection point, the surface excess Γ is estimated through the Gibbs equation: $\Gamma = -\frac{1}{RT}\frac{d\gamma}{d\ln C_f}$, for nonionic surfactants in dilute solutions where C_f corresponds to the free (or monomer) surfactant concentration. Assuming that HD (or NT)–PVA equilibrium follows a phase separation model, the concentration of HD (or NT)–PVA associating species is, thus, constant, and the HD or NT concentrations required for the complete formation of associating species are respectively 122.8 10^{-3} and 10.1 10^{-3} mol L^{-1}. Then, $C_f = C - \zeta$ where ζ=122.8 10^{-3} mol L^{-1} for HD and 10.1 10^{-3} for NT. Considering now that γ varies linearly with C as C is close to but lower than CMC ($\gamma = a + b\ln C$), the Gibbs equation becomes: $\Gamma = -\frac{1}{RT}\frac{d\gamma}{d\ln C_f} = -\frac{1}{RT}\frac{bC_f}{(C_f+\varsigma)} = -\frac{b}{RT}\left(1-\frac{\varsigma}{C}\right)$, and at C = CMC: $\Gamma_{CMC} = -\frac{b}{RT}\left(1-\frac{\varsigma}{CMC}\right)$. The determination of Γ_{CMC} allows also the determination of the interfacial molecular area A according to $A = \frac{1}{N_A \Gamma_{CMC}}$ where N_A is the Avogadro's number. Application of these equations to NT–water (w) and NT–PVA–w leads to $A_{NT/w}$= 50.1 10^{-20} m^2 and $A_{NT/PVA/w}$=47.6 10^{-20} m^2. Similarly, we obtain for the systems involving HD: $A_{HD/w}$=78.2 10^{-20} m^2 and $A_{HD/PVA/w}$=97.0 10^{-20} m^2. In pure water, the $A_{NT/w}$ value is twice lower than $A_{HD/w}$, whereas the polar head of NT is 1.5 times higher than that of HD. Such a peculiar behavior can be attributed to the NT alkyl chain, which is also 1.5 times longer than HD one, thus, contributing to higher hydrophobic interactions and to higher packing of the NT molecules at the air–water interface. Moreover, the higher number of –OH groups in NT molecules may also contribute to a better order of the NT molecules, thus, leading to a smaller molecular area than HD one. Examining now the influence of PVA on the molecular areas, a slight decrease of A is noticed in the NT–PVA system whereas an A increase is noticed in the HD–PVA system. PVA macromolecules can, then, take part differently to the adsorption of NT or HD and to the organization of the surfactant molecules at the air–water interface. On one hand, PVA contributes to the packing of the adsorbed NT molecules, and on the other hand, HD–PVA interacting species transfer from bulk solution to the interface in a less organized state. Hence, HD appears to be not sufficiently hydrophobic to maintain a strong packing at the interface as NT does in presence of PVA. Finally, tensiometry reveals interactions between PVA and nonionic polyol surfactants before micellization, and micellization does not seem to be affected by the presence of PVA. The observation of no change in surfactant CMC upon addition of polymer is in agreement with previous studies involving different nonionic polymer–nonionic surfactant–water systems such as polyacrylamide–Triton X-100–water [12], poly(vinyl alcohol)–poly(vinyl acetate) copolymer or poly (*N*-vinylpyrrolidone)–*n*-octyltriethylene glycol ether–water and (hydroxypropyl)cellulose or poly(ethylene oxide) or

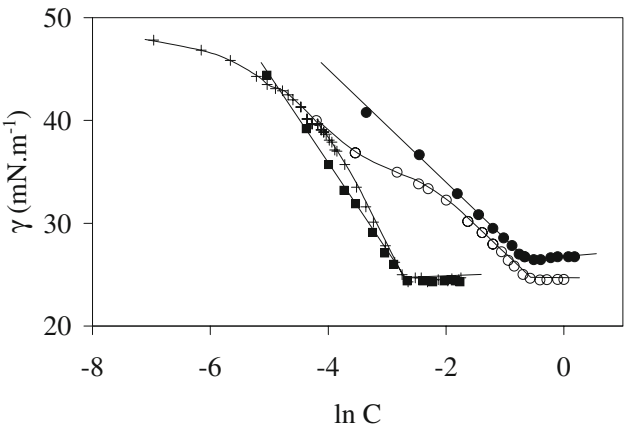

Fig. 4 Plots of the surface tension γ as a function of the polyol concentration C (*dark circles*: HD–water at 30 °C; *white circles*: HD/PVA (4.5 g L^{-1})–water at 30 °C; *dark squares*: NT–water at 45 °C; *crosses*: NT–PVA (4.5 g L^{-1})–water at 45 °C)

poly(propylene oxide)–*n*-octyl thioglucoside–water [40]. To further evidence the PVA–surfactant interactions and to complete the hydrodynamic dimension variations of PVA issued from dynamic light scattering measurements, where only a 1 to 2 nm radius variation is noticed in presence of HD, our investigation has been, then, focused on the viscosity study of PVA in presence of HD in water. Such a method permits us to follow indirectly the variations of the PVA hydrodynamic volume (instead of R_h determined by dynamic light scattering) through the variations of the intrinsic viscosity [η], which is proportional to the effective flowing volume V_e according to the equation $[\eta] = 2.5\frac{V_e}{M}$. Introducing the ratio $r = \frac{R_v}{R_h} = \left(\frac{V_v}{V_h}\right)^{1/3}$, we have $[\eta] = \left(\frac{10}{3}\frac{\pi N_A r^3}{M}\right)R_h^3$, and a ΔR_h variation of R_h leads to: $\frac{\Delta[\eta]}{[\eta]} = 3\frac{\Delta R_h}{R_h}$. Then, the examination of [η] should enable a three times magnification of the R_h variations. In the present work, for ΔR_h=1–2 nm and $R_h \cong 13$ nm, we can expect a relative variation of [η] around 25% to 50%. Considering the binary system polyol–water as solvent of PVA, the linear variation of the reduced viscosity η_{red} as a function of the polymer concentration C_{PVA} permits the determination of [η]. Such a study has been undertaken with HD–water solvents at various HD concentrations (see Fig. 2 for C_{HD}=0.6 mol L^{-1} as example). The influence of C_{HD} on [η] is shown on Fig. 5a. For the same HD concentration range as that used in dynamic light scattering measurements, we notice the [η] values range from around 74 to 100 mL g^{-1} and, then, $\frac{\Delta[\eta]}{[\eta]}$ is around 35%, which is in good accordance with the predictions arising from dynamic light scattering results. The [η] vs. C_{HD} curve presents two steps: a sharp [η] increase up to C_{HD} around 0.75 mol L^{-1} followed by a slow [η] increase with C_{HD}. Whereas the C_{HD} value obtained at this break point is higher than that obtained by tensiometry, it remains in the CMC range values previously determined by other methods [26]. Similarly the influence of other polyol (NT, HpT, OT) or water solvents on the PVA viscosity behavior has been investigated. Some η_{red} vs. C_{PVA} curves are presented on Fig. 2 as examples and the variation of [η] with C_{NT} is shown on Fig. 5a with the [η] vs. C_{HD} curve.

Other polyols lead to similar [η] vs. C_{polyol} curves consisting of two linear parts intercepting closely at the CMC. The [η] increase reflects the expansion of the PVA macromolecules probably caused by the association of polyol single molecules to the macromolecular chain. Such an affinity between polyol and PVA is evidenced by the Huggins coefficient k_H that decreases from around 0.6 to a constant value 0.4 as the CMC is reached (see Fig. 5b for HD–PVA–water and NT–PVA–water as examples).

Similarly to the procedure described in [41] to get information on the hydration of poly(ethyleneglycol)s by determination of solvation numbers h (number of moles of bonded water molecules in the inner hydration sphere per mole of macromolecular solute) from the change of solution viscosity with polymer concentration: $h = \frac{\rho_w}{M_w}\overline{M}_P\left(\frac{[\eta]}{2.5} - \overline{v}_p\right) = \frac{\rho_w}{M_w}\overline{M}_P\overline{V}_w$where ρ_w, M_w, and $\overline{V}_w$are the density, molar mass, and volume of w bound per gram of polymer (P), and [η], $\overline{M}_P$ and $\overline{v}_P$ are the intrinsic viscosity, molar mass, and apparent specific volume of the polymer defined by $\overline{v}_P = \frac{V_e}{M_P} - \overline{V}_w$, we evaluate the affinity between PVA and solvent molecules M through a coefficient $K_{M,T} = \frac{C_{M,PVA}}{C_{M,bs}}$ which describes the partition of M between the PVA microenvironment of molar volume V_e and M in the bulk solution (bs): $(M)_{bs} = (M)_{PVA}$. For aqueous polymer solutions at infinite polymer dilution, $C_{M,bs}$ becomes identical to C_M. In the case of the PVA–water system, $K_{w,T} = \frac{C_{w,PVA}}{C_w} = \frac{h/V_e}{C_w}$ where $h/V_e = \frac{\rho_w}{M_w}\left(1 - \overline{v}_P\overline{M}_P/V_e\right)$ and the apparent specific volume of PVA, $\overline{v}_P$, is approximately equal to 0.7893 cm^3 g^{-1} [14]. Such an approximation is based on volumetric results obtained in the case of concentrated aqueous PEG solutions: a maximum relative difference between $\overline{v}_{PEG}$ and its specific amorphous volume is 6.6% at a PEG concentration of 29 g L^{-1}. Given $V_e = [\eta]\frac{M_v}{2.5}$, we obtain: $K_{w,30\,°C} = 0.973 \pm 0.002$. In presence of polyol M in the monomer state in water, we estimate $K_{M,30\,°C} = \frac{C_{M,PVA}}{C_M}$ where $C_{M,PVA}$ =

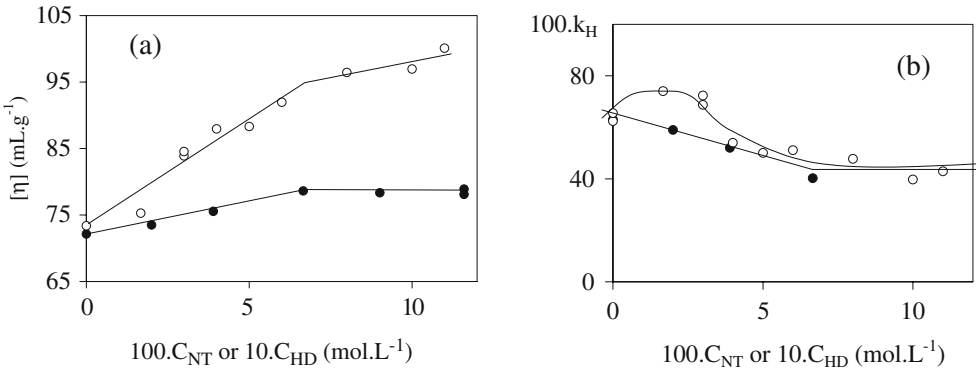

Fig. 5 Effect of C_{HD} or C_{NT} on the PVA intrinsic viscosity [η] (**a**) or Huggins coefficient k_H (**b**) in HD–water solvents at 30 °C (*white circles*) or in NT–water solvents at 45 °C (*dark circles*)

$\frac{\rho_M}{M_M}\left(1-\frac{M_{PVA}}{\rho_{PVA}V_e}-\frac{M_w}{\rho_w}\frac{h}{V_e}+\Delta V^r\right)$ with ΔV^r the relative excess volume ($\Delta V^r = 0$ when volumes are additive). Moreover, $h/V_e = K_{w,T}C_w$ and $C_w = \frac{\rho_w}{M_w}\left(1-\frac{C_M M_M}{\rho_M}+\Delta V^r\right)$ with M_M and ρ_M the respective molecular weight and the density of M. Then, the combination of these last equations leads to: $\frac{1}{[\eta]} = \frac{1}{2.1}\left[(1-K_{w,T})(1+\Delta V^r)-\frac{M_M}{\rho_M}(K_{M,T}-K_{w,T})C_M\right]$. From volumetric results about HD and water mixtures [42], ΔV^r varies with C_{HD} (mol L^{-1}) as: $\Delta V^r = -5.2\ 10^{-3} + 3.8\ 10^{-4}\ C_{HD}$. Then, in the polyol concentration range used: $\Delta V^r << 1$. In accordance with this model, the variations of $1/[\eta]$ as a function of C_M at temperature T are effectively linear as soon as C_M < CMC. Application of this model gives $K_{M,T}$ from the determination of the absolute slope of $1/[\eta]$ vs. C_M. To investigate the interactions between monomer M and PVA, the effect of the polyol structure on $K_{M,T}$ is examined. Our results are, thus, compared to those previously obtained from PVA viscosity studies with various monoalcohols or water mixtures used as solvents [17, 18]. From these viscosity results, the $K_{M,T}$ values of ethanol, 1-propanol, and 1-butanol at 25 °C have been, then, calculated according to the present model. The variations of $K_{M,T}$ with the molecular weight M of the monoalcohols and the polyols are illustrated on Fig. 6a.

The temperature T has only a weak effect on $K_{M,T}$ as it is shown for HD at 30 °C and 45 °C. To further estimate the contribution of the different groups of the mono- or polyols on their association with PVA, their effect on the standard Gibbs free energy $\Delta_{bs,PVA}G^0_{M,T} = -RT\ln K_{M,T}$ corresponding to the transfer of M from the bulk solution (bs) to the PVA microenvironment has been examined. Taking into consideration the contribution of each polyol group to $\Delta_{bs,PVA}G^0_{M,T}$, this thermodynamic parameter can be expressed as: $\Delta_{bs,PVA}G^0_{M,T} = \Delta_{bs,PVA}G^0_{CH_3,T} + (n_C-1)\ \Delta_{bs,PVA}G^0_{CH_2,T} + \Delta_{bs,PVA}G^0_{polar\ head,T}$ where n_C is the carbon atom number of the polyol alkyl chain. For the monoalcohols and the triols series, the $\Delta_{bs,PVA}G^0_{M,T}$ values have been reported as a function of n_C (see Fig. 6b) and lead to: $\Delta_{bs,PVA}G^0_{CH_2,T} = -156 \pm 34$ and -198 ± 91 J mol^{-1} in monoalcohols and triols, respectively. Such values are on the same order of magnitude. By adding on one hand one –CH_2- and –CHOH-pair group successively on 1-butanol and on HD, and on the other hand two –CH_2 and one –CHOH groups on 1-propanol and on HD, we estimate: $\Delta_{bs,PVA}G^0_{CHOH,T} = 162 \pm 94$ J mol^{-1}. Despite the high incertitude on $\Delta_{bs,PVA}G^0_{CHOH,T}$, its positive value reflects an unfavorable transfer process of the –CHOH group from the bulk solution to the PVA microenvironment, and the negative value of $\Delta_{bs,PVA}G^0_{CH_2,T}$ is consistent with a rather favorable transfer of the –CH_2 groups from the bulk solution to the PVA microenvironment. Then, the presence of –OH groups in PVA and in polyols does not contribute favorably to the interactions between PVA and the polyols. Hydrophobic interactions are most involved in such weakly interacting systems.

Conclusion

Dynamic light scattering and tensiometry have first evidenced the existence of interactions between various polyols and PVA. From dynamic light scattering, the variation of R_h becomes noticeable as the polyol concentration exceeds its CMC, whereas noticeable effects of PVA on the polyol–water surface tension are mostly observed as the polyol concentration is far lower than its CMC (around 5% to 25% of the CMC). Then, interactions between polyols and PVA in water can occur in a large polyol concentration beginning at around 5% of its CMC. The interactions have been, then, evidenced and quantitatively examined by viscosimetry. From the intrinsic viscosities $[\eta]$ of PVA in polyol–water solvents, the corresponding $1/[\eta]$ variations with polyol concentration enable the introduction of a constant $K_{M,T}$ characteristic of the polyol (M) partition between the bulk solution (bs) and the close microenvironment of PVA macromolecules whose dimension is defined by its flowing volume. The corresponding Gibbs free

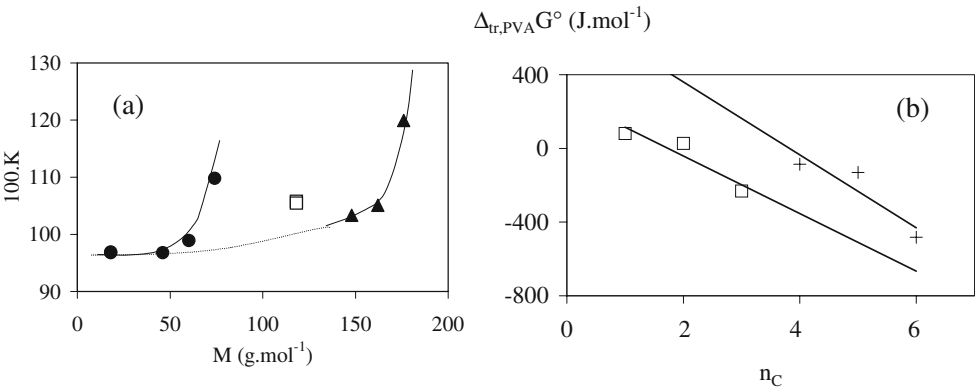

Fig. 6 **a** Effect of the molecular weight M of monoalcohols (*dark circles*), HD (*white squares*), and triols (*dark triangles*) on the $K_{M,T}$ constant; **b** effect of the carbon atom number n_C of the monoalcohol alkyl chain (*white squares*) and of the triol alkyl chain (*crosses*) on the Gibbs free energy of transfer of the M species from the bulk solution to the PVA microenvironment $\Delta_{bs,PVA}G^0_{M,T}$

energy of polyol transfer from (bs) to PVA microenvironment $\Delta_{bs,PVA}G^0_{M,T}$ is, thus, deduced, and the –(CH_2)- and –CHOH-group contributions to $\Delta_{bs,PVA}G^0_{M,T}$are determined. The results indicate on one hand an unfavorable contribution of –CHOH groups to the polyol–PVA interactions, despite the presence of –OH groups in both polyol and PVA. On the other hand, the –CH_2 groups of polyols appear to interact favorably with PVA, probably through its hydrocarbon skeleton. Moreover, the –CH_2 groups, which present no affinity with water molecules, are repelled from the aqueous bulk solution to the PVA microenvironment. The thermodynamic contributions to $\Delta_{bs,PVA}G^0_{M,T}$, thus, estimated result from competitive interactions between –CHOH groups and water, and between –CHOH groups and PVA for $\Delta_{bs,PVA}G^0_{CHOH,T}$ and competitive –CH_2–water and –CH_2–PVA interactions for $\Delta_{bs,PVA}G^0_{CH_2,T}$.

References

1. Rosen O, Sjöström J, Pieulell L (1998) Langmuir 14:5795
2. Marques EF (1999) J Chem Phys 57:4814
3. Tsianou M, Alexandridis P (2005) Surfactant-polymer interactions, mixed surfactant systems. In: Abe M, Scamehorn JF (eds) Surfactant science series. vol. 124. Dekker, New York, pp 657–707
4. Brown W, Fundin J, Miguel MdaG (1992) Macromolecules 25:7192
5. Xia J, Dubin PL, Kim Y (1992) J Phys Chem 96:6805
6. Witte FM, Engberts JBJN (1988) J Org Chem 53:3085
7. Ruckenstein E, Huber G, Hoffmann H (1987) Langmuir 3:382
8. Goddard ED, Ananthapadmanabhan KP (1993) Interactions of surfactants with polymers and proteins. CRC, Boca Raton
9. Zana R, Benrraou M (2000) J Colloid Interface Sci 226:286
10. Maltesh C, Somasundaran P (1992) Colloids and Surfaces A 69:167
11. Saito S (1987) Nonionic surfaisants. In: Shick MJ (ed) Polymer-surfactant interactions. Dekker, New York, p 881
12. Mya KY, Jamieson AM, Sirivat A (1999) Polymer 40:5741
13. Morita R, Honda R, Takahashi Y (2000) J Controlled Release 68:115
14. Finch CA (1973) Polyvinyl alcohol, properties and applications. Wiley, New York
15. Kim IT, Luckham PF (1991) J Colloid Interface Sci 144:174
16. Finch CA (ed) (1992) In: Polyvinyl alcohol—developments. Wiley, New York
17. Wolfram E, Nagy M (1969) Annales Universitatis Scientiarum Budapetinensis de Rolando Eotvos Nominatae, Sectio Chemica 11:57
18. Wardlaw GC, Humphrey S, Eagland D (1977) Br Polymer J 9:278
19. Swern D, Billen GN, Scanlan JT (1946) J Amer Chem Soc 68:1504
20. Durand RR, Hajii SM, Coudert R, Cao A, Taillandier E (1988) J Phys Chem 92:1222
21. Coudert R, Hajii SM, Cao A (1993) J Colloid Interface Sci 155:173
22. Huggins ML (1942) J Amer Chem Soc 64:2716
23. Kaemer EO (1938) J Ind Eng Chem 30:1200
24. Mead DJ, Fuoss RM (1942) J Amer Chem Soc 64:277
25. Koppel DE (1972) J Chem Phys 57:4814
26. Damas C, Naejus R, Coudert R, Frochot C, Brembilla A, Viriot ML (1998) J Phys Chem B 102:10917
27. Hajii SM, Errahmani MB, Coudert R, Durand RR, Cao A, Taillandier E (1989) J Phys Chem 93:4819
28. Matsumoto M, Imai K (1957) J Polym Sci 24:125
29. Lewandowska K, Staszewska DU, Bohdanecky M (2001) Eur Polym J 37:25
30. Beresniewsky A (1959) J Polym Sci 39:63
31. Flory PJ, Leutner FS (1948) J Polym Sci 3:880
32. Flory PJ, Leutner FS (1950) J Polym Sci 5:267
33. Tacx JCJF, Schoffeleers HM, Brands AGM, Teuwen L (2000) Polymer 41:947
34. Nakajima A, Furudati K (1949) Kobunshi Kagaku 6:460
35. Schulz GV (1939) Z Physik Chem B43:25
36. Douglas JF, Roovers J, Freed KF (1990) Macromolecules 23:4168
37. Park IH, Choi EJ (1996) Polymer 37:313
38. Flory PJ (1953) Principles of polymer chemistry. Cornell University Press, Ithaca
39. Park S, Chang T, Park IH (1991) Macromolecules 24:5729
40. Brackman JC, Van Os NM, Engberts JBFN (1988) Langmuir 4:1266
41. Kirinčič S, Klofutar C (1999) Fluid Phase Equilibria 155:311
42. Romero CM, Páez MS, Arteaga JC, Romero MA Negrete F (2007) J Chem Thermodynamics 39:1101